Applied Clay Science 174 (2019) 69–76

Contents lists available at ScienceDirect

Applied Clay Science

journal homepage: www.elsevier.com/locate/clay

Research paper

H_2-fuelled microbial metabolism in Opalinus Clay

Aislinn A. Boylan[a,*,1], Carla Perez-Mon[a,1,2], Laurent Guillard[a], Niels Burzan[a], Luca Loreggian[a], Markus Maisch[b], Andreas Kappler[b], James M. Byrne[b], Rizlan Bernier-Latmani[a]

[a] Environmental Microbiology Laboratory, École Polytechnique Fédérale de Lausanne, Lausanne 1015, Switzerland
[b] Eberhard Karls Universitaet Tuebingen, Center for Applied Geoscience (ZAG), Sigwartstrasse 10, Tuebingen 72076, Germany

ARTICLE INFO

Keywords:
Opalinus Clay
Deep geological repository
Sulfate-reducing bacteria
Geomicrobiology
Nuclear waste

ABSTRACT

In Switzerland, the Opalinus Clay formation is considered the most likely host rock for a deep geological repository for nuclear waste. In deep geological repositories, H_2 is expected to be the most abundant gas formed from the degradation of waste and from metal corrosion. The microbial community present in Opalinus Clay is capable of utilizing H_2 as an electron donor and sulfate as an electron acceptor to produce hydrogen sulfide. This could be problematic due to its potential for increasing the corrosion of metal waste canisters containing radioactive waste, however, the possible impacts of these processes on the clay rock have not been fully investigated. In this study, a series of microcosm experiments were set-up containing Opalinus Clay and porewater from the Mont Terri underground research laboratory (Switzerland) as an inoculum. Uninoculated microcosms were established to investigate abiotic processes.

In the presence of clay, a higher aqueous sulfate concentration was detected than in those with only porewater present and this concentration decreased over time in the inoculated experiments. However, there was no evidence of hydrogen sulfide production in the aqueous phase. In all experiments with clay, there was an increase in aqueous Fe^{2+} concentrations with the highest concentrations found in uninoculated experiments. The sulfur speciation of the Opalinus Clay was analysed and the results of the inoculated sample suggested that hydrogen sulfide reacted with Fe^{2+}, precipitating iron sulfide minerals. After the incubation period, the microbial community was dominated by the sulfate-reducing *Desulfobulbaceae* family.

The study suggests that H_2-fuelled, microbially-mediated sulfate reduction can affect the mineral composition within the Opalinus Clay due to the precipitation of iron sulfide minerals. These precipitation reactions may enhance the long-term integrity of the repository by removing corrosive hydrogen sulfide from solution when sufficient Fe^{2+} is available and so protecting the canisters containing the nuclear waste.

1. Introduction

Deep geological repositories (DGRs) are widely accepted as the most viable concept for the long-term disposal of intermediate- and high-level nuclear waste (IAEA, 2003). Due to the extremely long half-lives of some of the radionuclides held within the waste (*e.g.*, ^{79}Se half-life = 3.27×10^5 a; ^{99}Tc half-life = 2.1×10^5 a; ^{129}I half-life = 1.57×10^7 a; ^{135}Cs half-life = 3×10^6 a (NCRP, 1978)), it is necessary for the material to be contained for hundreds of thousands of years. Therefore, repository designs are based on using a stable geological environment, the deep subsurface, to mitigate the risks posed by radioactive materials to human health (Bagnoud et al., 2016a; IAEA, 2003). A variety of rock formations are being considered across the globe with Finland having already started the excavation process to place a repository within granitic bedrock (STUK, 2017). Other European nations are focusing on sedimentary rock, in particular clay formations such as Opalinus Clay (Switzerland), Boom Clay (Belgium) and Callovo-Oxfordian Clay (France) (Bagnoud et al., 2016b; Bengtsson and Pedersen, 2016; Nagra, 2008; Stroes-Gascoyne et al., 2007). Clay formations have small pore sizes (0.01–0.02 μm for Opalinus Clay (Pearson et al., 2003)), which limit the movement of water and growth of microorganisms, making them favourable host rocks as well as the primary constituent of many potential engineered barriers (Leupin et al., 2017). Switzerland has been investigating the suitability of the Opalinus Clay formation for DGR for several decades, with many studies undertaken in the underground research laboratory (URL) at Mont

* Corresponding author.
E-mail address: aislinn.boylan@epfl.ch (A.A. Boylan).
[1] These authors contributed equally to this work.
[2] Present address: Swiss Federal Institute for Forest, Snow and Landscape Research WSL, Zürcherstrasse 111, 8903 Birmensdorf, Switzerland.

https://doi.org/10.1016/j.clay.2019.03.020
Received 7 December 2018; Received in revised form 5 March 2019; Accepted 18 March 2019
Available online 28 March 2019

Terri, Saint-Ursanne (Bagnoud et al., 2016a, 2016c; Houben et al., 2014; Leupin et al., 2017; Stroes-Gascoyne et al., 2007; Thury, 2002). In the Swiss high level waste repository concept, the nuclear waste will be contained within steel canisters, which will then be surrounded by a bentonite clay backfill situated within the Opalinus Clay host rock (Nagra, 2002).

The microbial communities that exist in these deep subsurface environments may impact the stability of geological repositories. One important factor is their ability to both produce and consume gases including H_2, CO_2 and CH_4. The production of a large amount of gas through anaerobic corrosion of metals or the microbial fermentation of organic compounds within nuclear waste poses a risk because of the potential damage it could cause to the structural integrity of the repository, including the surrounding rock. In particular, H_2 is of importance due to its abundant production from the anaerobic corrosion of nuclear waste-containing steel canisters within the repository (Bagnoud et al., 2016a; Libert et al., 2011; Lin et al., 2005a, 2005b; Vinsot et al., 2014).

The construction of repositories will result in the introduction of oxygen, water, space and nutrients, all of which could encourage the growth of indigenous facultative anaerobes as well as introduce an exogenous community (Leupin et al., 2017). After closure of the repository, it is expected that reducing conditions will recur. Sulfate reduction and methanogenesis are possible terminal electron accepting processes (TEAPs), with hydrogenotrophic sulfate reduction able to reduce gas volume to a greater extent than methanogenesis (Bagnoud et al., 2016c). Furthermore, microbial activity can lead to physical and chemical changes in the host rock including the leaching of specific elements, and may enhance or retard the transport of radionuclides and the dissolution or precipitation of mineral phases. These processes may have a profound impact on the safety case for the repository due to a reduction in the integrity of the host rock or the engineered barrier system.

Amendment with H_2 stimulated sulfate-reducing bacteria (SRB) in a water-filled borehole within Opalinus Clay as shown by an *in-situ* borehole experiment at Mont Terri URL (Bagnoud et al., 2016a). Hydrogenotrophic sulfate reduction occurs according to:

$$4H_2 + SO_4^{2-} \rightleftharpoons S^{2-} + 4H_2O \quad (1)$$

Within DGR environments where the pH is likely to exceed a value of 8, S^{2-} will exist as HS^- (Pedersen et al., 2017) which is of concern due to its ability to corrode the steel canisters in which the waste will be placed. HS^- is also able to reduce Fe (III) coupled to the partial oxidation of HS^- to produce Fe^{2+} and elemental sulfur (S_0):

$$HS^- + 2Fe^{3+} \rightleftharpoons 2Fe^{2+} + S_0 + H^+ \quad (2)$$

This process can release Fe^{2+} into the porewater, which can react with HS^- to form iron sulfide minerals:

$$HS^- + Fe^{2+} \rightleftharpoons FeS + H^+ \quad (3)$$

Sources of Fe(III) include iron within clay mineral structures or other Fe(III)-bearing minerals (Pentráková et al., 2013; Pyzik and Sommer, 1981), for example of the backfill or host rock. There is also evidence to suggest that Fe(III) may be released from the steel nuclear waste-containing canisters due to corrosion (Smart et al., 2001). Fe(III) in mineral structures can be reduced directly by microorganisms where there is sufficient space and water available. In particular, a previous study by Kostka et al. (1999), suggested that the bioreduction of Fe(III) to Fe(II) in phyllosilicate clay minerals reduces the surface area, decreases clay swelling and causes the phyllosilicate structure to collapse. Specifically, the structure of bentonite (utilized as the engineered barriers in most DGRs) has been found to be altered due to SRB activity where the reduction of Fe(III) within the mineral structure can have a destabilizing effect on the dioctahedral smectites (Lantenois et al., 2005; Pedersen et al., 2017). This may have significant implications in the DGR environment as these alterations could weaken the clay structure, creating fractures that would facilitate microbial growth and radionuclide transport.

A previous *in-situ* study by Bagnoud et al., (2016a), at the Mont Terri URL examined the ability of microbial populations within the porewater of the Opalinus Clay to utilize H_2 as the electron donor. The aqueous geochemical results of the study suggested that there was an initial increase of Fe^{2+} concentration, after which Fe^{2+} disappeared from solution. At a similar time point, the concentration of HS^- in solution began to increase suggesting a possible interaction between sulfur and iron. However, no analysis of the solid phase was possible during this study.

The aim of the present study is to determine the speciation of iron and sulfur in Opalinus clay after exposure to sulfate-reducing bacteria and to consider the implications this may have on the DGR safety case.

2. Materials and methods

2.1. Opalinus Clay

A core from the sandy facies of the Opalinus Clay geological formation at Mt. Terri Rock Laboratory (St-Ursanne, Switzerland) was recovered during the drilling of BMA-A2 borehole, with pressurized air used as the drilling fluid. A section of the core was separated using a circular saw immediately after extraction, the core was then conditioned in Mylar® bags and stored at −80 °C until use. After removal from the freezer, the core was split apart using hammer and chisel under sterile, oxic conditions. Clay from the interior of the core was recovered under sterile conditions using a scalpel and then placed immediately in to N_2-filled serum bottles.

2.2. Experimental set up

Duplicate microcosms were set-up in 200 mL serum bottles containing either 40 g*L^{-1} or 20 g*L^{-1} of Opalinus clay from the BMA-A2 borehole. To these, 90 mL of artificial porewater (APW, modified from Pearson et al., 2007) and 1 mL of 0.1% resazurin dye was added. The APW was autoclaved prior to addition to the serum bottles (see Table 1 for APW composition). An additional set of duplicate bottles contained the APW and resazurin dye. All bottles were flushed with sterile N_2 for 30 min and then flushed with a sterile H_2:N_2 mix (20:80%) for 10 min. 10 mL of porewater was added as an inoculum to all bottles (taken from borehole BPC-C2, Mont Terri, Saint-Ursanne, Switzerland). Single control experiments were set up containing only 100 mL of APW and resazurin dye. All setup and handling was done under sterile conditions. This resulted in four experimental conditions: i) clay – inoculated; ii) clay – uninoculated; iii) no clay – inoculated, and iv) no clay – uninoculated, using two different amounts of clay. Microcosm bottles were incubated in the dark at 19 °C for the duration of the experiment (136 days).

2.3. Geochemical analyses

Periodically 3 mL aliquots were taken from the aqueous phase of

Table 1
Composition of the artificial porewater (APW). Modified from Pearson et al., 2003 with sodium sulfate replaced by sodium chloride.

Compound	Amount (g/L)
KCl	0.16
$MgCl_2.6H_2O$	4.68
$CaCl_2.2H_2O$	2.78
NaCl	30
$NaHCO_3$	0.042
pH	8.0

each bottle using a needle and N_2-filled syringe to retain anoxic conditions, the sample volume was replaced with N_2 gas to retain overpressure in the bottles. The sample was immediately filtered using a 0.22 µm filter to remove any microbes and clay particles. For aqueous Fe^{2+} measurement, filtered aliquots were stored in 1 M HCl to preserve Fe(II). Ferrous iron analysis was conducted on a UV–vis spectrophotometer (UV-2501PC, Shimadzu Co., Japan) using the photometric Ferrozine assay (Stookey, 1970). The samples were left to develop for 20 min prior to measurement at 562 nm. Samples for sulfide measurement were added to Eppendorf tubes containing zinc acetate (final concentration 1%) to preserve sulfide. Subsequently, sulfide concentrations were also measured using UV–vis spectrophotometry according to a published method (Cline, 1969). Sulfate was measured using an ion chromatograph equipped with an IonPac AS11-HC column (DX-3000, Dionex, USA) and with a KOH gradient from 0.5 to 30 mM for the elution. At the same time points as the aqeous samples, 3 mL gas samples were taken from the headspace of the bottles and injected directly in to a gas chromatograph with flame ionization detector (GC-FID, Varian 450-GC, Agilent, Santa Clara, USA) to measure the H_2 concentrations. An additional 3 mL of N_2 gas was added to bottles to replace the gaseous volume taken. Solution pH was measured periodically in experiments by an Orion 815,600 ROSS Combination pH electrode (ThermoScientific), calibrated daily at pH values of 4, 7 and 10.

At the end of the experiment, replicate samples were combined into four groups prior to filtration to ensure sufficient DNA recovery for sequencing: i) clay – inoculated; ii) clay – uninoculated; iii) no clay – inoculated, and iv) no clay – uninoculated. The aqueous phase was decanted from the microcosm bottles to separate it from the clay. The solution was then filtered using 0.1 µm polycarbonate filters (0.1 µm filters used at end time point to retain sufficient biomass for sequencing due to the lower aqueous volume compared to the original porewater where 0.22 µm filter was used). Filters were placed in 1.5 mL Eppendorf tubes containing 500 µL of Lifeguard preservation solution (QIAGEN) and stored at −20 °C prior to DNA extraction. The solid phase clay samples were dried under vacuum in anoxic conditions, the clay was then ground to a fine powder using pestle and mortar and transferred to 10 mL serum bottles to maintain anoxic conditions prior to spectroscopic analyses.

2.4. Microbial community

Porewater was extracted from the BPC-2 borehole at Mont Terri URL (Saint-Ursanne, Switzerland) and collected in a sterile 1 L N_2-filled serum bottle to maintain anoxic conditions. It was stored overnight at 4 °C prior to use. It was checked for living cells using SYBR Green nucleic acid stain (Sigma-Aldrich, USA) on an epifluorescence microscope. For preparation, 1 mL of sample was filtered on a black polycarbonate membrane (0.22 µm), rinsed three times with phosphate-buffered saline solution, and finally stained with a solution of SYBR Green I (1:200 dilution) and polyvinylalcohol (moviol) (Lunau et al., 2005). 900 mL of BPC-2 borehole water was filtered through a 0.22 µm pore size filter and the filter was retained for DNA analysis to determine the composition of the original microbial community.

DNA was extracted from four supernatant samples from i) clay – inoculated; ii) clay – uninoculated; iii) no clay – inoculated, iv) no clay – uninoculated, as well as (v) the original BPC-2 borehole water sample. Extractions were undertaken using a previously described phenol-chloroform-isoamlyalcohol extraction followed by a glycogen-assisted ethanol precipitation (see Bagnoud et al., 2016a for detailed methodology). Of these, only two samples yielded sufficient DNA for sequencing: the inoculated clay sample and the original borehole sample. For full description of method see supplementary information, section S1.

2.5. X-ray absorption sulfur XANES

S K-edge X-ray analysis of the near edge structure (XANES) spectra were collected from the clay samples at Stanford Synchrotron Radiation Lightsource (Menlo Park, CA), at beam line 4–3. Measurements were conducted in fluorescence mode on ground sediments using a Vortex® 4-element solid-state Si drift detector (Hitachi High-technologies Science, USA). The energy for S K-edge was calibrated at the first inflection point of a sodium thiosulfate standard (2472 eV). Multiple XANES spectra were averaged to improve signal-to-noise ratio, normalized and background-subtracted using Athena (Ravel and Newville, 2005). Linear combination fitting (LCF) was used to analyse the spectra and assign mineral phases, details of data processing are provided in the supplementary information, S2.

2.6. ^{57}Fe Mössbauer spectroscopy

Three clay samples were analysed for Fe speciation using Mössbauer spectroscopy: an unaltered sample of the source rock, a sample taken at the endpoint of the inoculated experiments, and a sample from the endpoint of the uninoculated experiments. Within an anoxic glovebox (100% N_2), samples were loaded into Plexiglas holders (area 1 cm^2), forming a thin disc. Sample holders were transported to the instrument within airtight bottles which were only opened immediately prior to loading into a closed-cycle exchange gas cryostat (Janis cryogenics) under a backflow of He to minimize exposure to air. Spectra were collected at 77 K and 5 K using a constant acceleration drive system (WissEL) in transmission mode with a ^{57}Co/Rh source. All spectra were calibrated against a 7 µm thick α-^{57}Fe foil that was measured at room temperature. Analysis was carried out using Recoil (University of Ottawa) and the Voigt Based Fitting (VBF) routine (Rancourt and Ping, 1991). The half width at half maximum (HWHM) was constrained to 0.134 mm/s during fitting.

2.7. Geochemical modelling

Geochemical modelling was performed using PHREEQC (version 3.4) geochemical speciation program (Parkhurst and Appelo, 2013) with the PHREEQC database to determine the saturation indices for the major mineral phases within Opalinus Clay and corresponding concentrations of Fe^{2+} and SO_4^{2-} in solution (see supplementary information S3).

3. Results

3.1. Geochemical analyses

A decrease in the aqueous sulfate concentration was observed in both 40 g*L^{-1} and 20 g*L^{-1} inoculated clay experiments, with most of the decrease occurring from 0 to 50 days of incubation (Fig. 1a,b). In the 40 g*L^{-1} inoculated experiment, the original sulfate concentration of 860 ± 103 µM decreased to 114 ± 2 µM by day 47. This concentration continued to decrease until it was below detection at 106 days and remained below detection (25 ± 5 µM) at the end of the experiment (134 days). In the 20 g*L^{-1} inoculated experiment, the initial concentration of sulfate was 500 ± 52 µM which decreased until it was below detection at 106 days, remaining below detection at the end of the experiment (134 days). For the inoculated experiments without clay present (Fig. 1c), the sulfate concentration remained consistent, with concentrations measured at 285 ± 55 µM throughout the experiment. For all uninoculated samples, the concentration of sulfate remained relatively consistent over time with 476 ± 74 µM measured for the duration of the 40 g*L^{-1} experiments, 199 ± 27 µM for the duration of the 20 g*L^{-1} experiments and 25 ± 5 µM for the duration of the experiments without clay present (corresponding to the detection limit of the technique). Thus, sulfate is derived from two sources, the

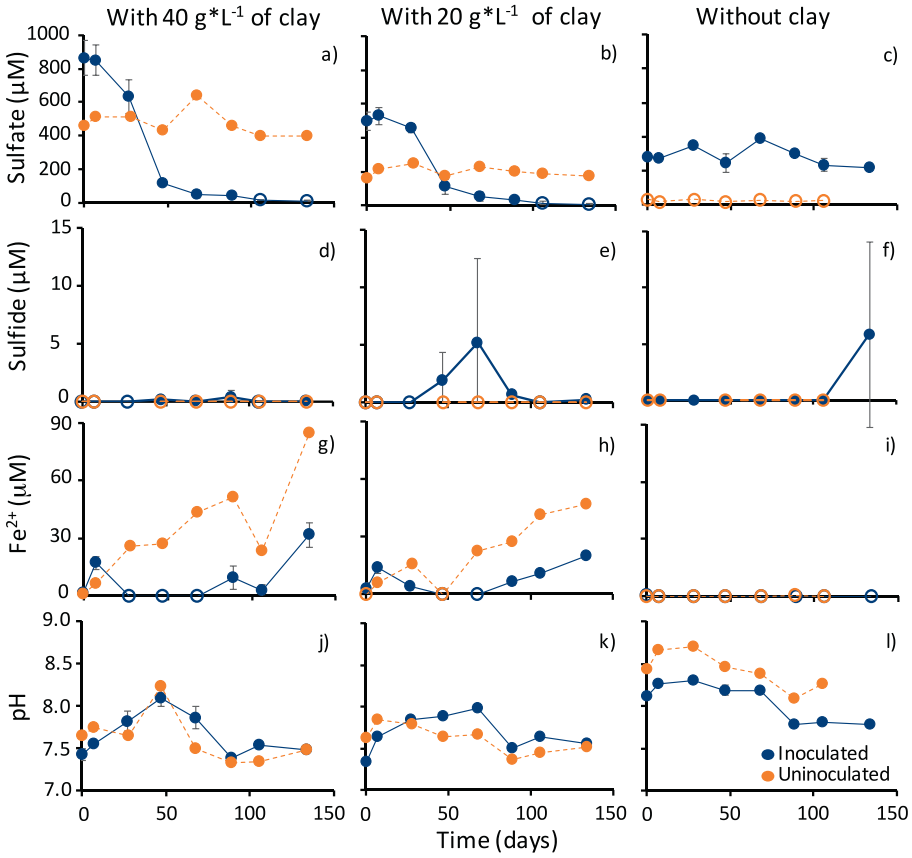

Fig. 1. Geochemical analyses of inoculated and uninoculated systems under three experimental conditions: with 40 g*L^{-1} of clay; with 20 g*L^{-1} of clay; and without clay: a,b,c) sulfate concentration; d,e,f) sulfide concentration; g,h,i) Fe^{2+} concentration; and j,k,l) pH. Inoculated samples shown in blue with a continuous line, uninoculated in orange with a dashed line. Unfilled data points represent values below the limit of detection for the method used. Error bars on the inoculated system (dark blue) denote the standard deviation of duplicate samples. Single samples were used for the uninoculated conditions. (For interpretation of the references to colour in this figure legend, the reader is referred to the web version of this article.)

clay rock and the porewater inoculum.

In the 40 g*L^{-1} experiments, the inoculated system showed no change in sulfide concentration for the duration of the experiment with concentrations < 0.4 µM (Fig. 1d). The concentration of sulfide in the inoculated 20 g*L^{-1} system remained relatively low with a maximum concentration of 5 ± 7 µM at 68 days and a final concentration of 0.3 ± 0.1 µM measured on day 134 (Fig. 1e). For the inoculated experiment without clay present, the concentration remained below the limit of detection (0.02 µM) until the final measurement of 6 ± 8 µM at 134 days (Fig. 1f). All sulfide concentrations for the uninoculated experiments were below the limit of detection for the duration of the experiments (106 days).

Aqueous Fe^{2+} concentrations in both the 40 g*L^{-1} and 20 g*L^{-1} clay experiments increased with time for both inoculated and uninoculated systems (Fig. 1g,h). In the 40 g*L^{-1} inoculated system, the initial concentration of Fe^{2+} was 2 ± 2 µM. On day 7, this has increased to 17 ± 3 µM before decreasing to 3 ± 3 µM on day 106. At the end of the experiment, a concentration of 32 ± 6 µM was measured. The concentration of Fe^{2+} in the uninoculated 40 g*L^{-1} system increased from an initial concentration of 1 µM to a final concentration of 85 µM at 134 days. The 20 g*L^{-1} inoculated system showed a similar pattern to the 40 g*L^{-1} inoculated: in the earlier time points (day 0 to day 89), the Fe^{2+} concentration fluctuated between 0 and 14 µM, however from day 89 on, there was a consistent increase in Fe^{2+} concentration from 6 ± 2 µM to 20 ± 2 µM at the end of the experiment (134 days). For the uninoculated 20 g*L^{-1} experiment, concentrations of Fe^{2+} increased from 0 µM at the initial time point to 15 µM on day 28. After decreasing to 0 µM on day 47 the concentration of Fe^{2+} then increased consistently with 47 µM measured at the end of the experiment (134 days). Without clay present, both the inoculated and uninoculated systems showed no Fe^{2+} in solution with all timepoints below the limit of detection (< 0.35 µM) (Fig. 1i), which suggests that the clay is the source of iron.

The pH values in the 40 g*L^{-1} inoculated system increased from 7.4 ± 0.1 on day 0 to 8.1 ± 0.1 on day 47 (Fig. 1j). The pH then decreased to 7.4 ± 0.1 on day 89, remaining at pH 7.5 ± 0.1 for the remaining duration of the experiment (day 134). In the uninoculated system, the pH on day 0 was 7.7, and increased to a maximum of 8.2 on day 47 before decreasing to 7.5 at the end of the experiment (day 134). For the 20 g*L^{-1} system, the initial pH was 7.3 ± 0.1, and increased to a maximum of 8.0 ± 0.04 on day 86 before decreasing to 7.5 ± 0.1 on day 89 with the final pH at 7.6 ± 0.1 at the end of the experiment (day 134)(Fig. 1k). In the uninoculated system, the pH value remained constant at 7.6 ± 0.3 for the duration of the experiment (134 days). Without clay present (Fig. 1l), the initial pH values were higher than those where clay was present for both the inoculated and uninoculated samples (pH 8.1 ± 0.01 and pH 8.4 respectively). The inoculated system showed an increase in pH to 8.3 ± 0.1 on day 28 before decreasing to 7.8 ± 0.1 by the end of the experiment (day 134). The uninoculated system showed a similar trend, increasing from 8.4 on day 0 to 8.7 on day 28 before decreasing to 8.3 at the end of the experiment (day 106).

The resazurin results for all inoculated samples with clay present suggest a consistent reducing environment, evidenced by the change in colour from blue (resazurin) to pink (resorufin, redox potential (Eh') ≤ −50 mV)) to clear (dehydroresorufin, Eh' ≤ −100 mV) (Vladimir and Igor, 2009). In the inoculated samples without clay, reducing conditions occured in only one of the duplicate samples, and occurred later in the experiment in comparison to those systems with clay present for the second replicate. For both clay-containing, uninoculated samples, the colour remained pink suggesting that low redox potential conditions remained prevalent for the experimental run but no further reduction of resorufin to dehydroresorufin took place. In the uninoculated experiment without clay, the colour remained blue, signaling the persistence of resazurin and indicating that high redox potential conditions persisted throughout the experiment due to limited

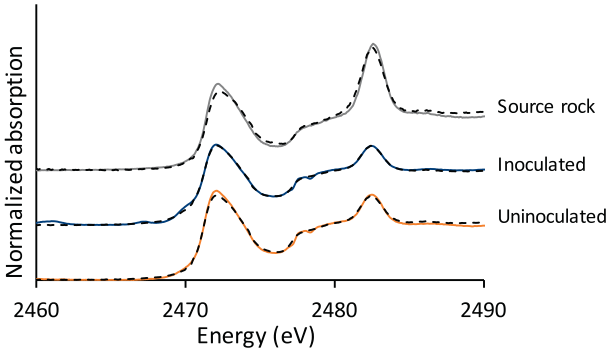

Fig. 2. Representative S edge XANES spectra for the source rock, inoculated and uninoculated clay samples. Dashed line represents linear combination fitting of mineral standards (see Table 2).

microbial activity within this sample and the absence of the reducing power of the clay rock.

The concentration of H_2 in the headspace of the experiment bottles remained at 11 ± 4% for the duration of the experiment under all experimental conditions (see supplementary information S4 for data set).

3.2. Sulfur XANES analysis

The S K edge XANES analysis of the inoculated and uninoculated clay samples show spectra with contributions from four sulfur species (Fig. 2). In all samples, pyrite and sulfate were identified. In the inoculated sample, three phases were identified: pyrite, sulfate, and a minor contribution of FeS (mackinawite) which was verified by comparison of the R-factor with and without the FeS standard spectra included in linear combination fitting (LCF, Table 2). In the uninoculated sample, the presence of elemental sulfur was also verified by R-factor comparison. Spectra for mineral standards used for LCF can be found in supplementary information, Fig. S1.

3.3. ^{57}Fe Mössbauer spectroscopy

Results of the ^{57}Fe Mössbauer spectroscopy analyses suggest that pyrite was present in all samples. In addition, the fitting parameters (supplementary information S5) indicate the abundance of at least two additional Fe(II) phases in each sample that likely correspond to an Fe (II) mineral and an Fe(II)-bearing phyllosilicate. The detection of pyrite was relatively consistent in all samples with around 30% relative abundance (Table 3). The additional unidentified Fe(II) phases detected slightly vary in their relative abundances ranging from approximately 25 to 45% respectively, perhaps due to the heterogeneity within Opalinus Clay.

3.4. Microbial community composition

Three phyla were identified from the analysis of the 16S rRNA sequences from the original borehole sample as well as the inoculated sample after incubation. These were Proteobacteria, Firmicutes and Actinobacteria. In the unaltered sample, 11 individual OTUs were identified, with 3 OTUs responsible for over 95% of the total reads (Fig. 3). After incubation the microbial community was composed of 9 OTUs (see supplementary data, Table S5 for complete OTU table). Of these OTUs, *Desulfobulbaceae* represented over 98% of the reads, a difference of 41% in comparison to the original, unaltered borehole sample.

Table 2
Sulfur containing phases identified by XANES shown as a percentage of total for inoculated and uninoculated samples. R-factor of < 0.05 suggests good fit with data. Number in brackets shows uncertainty in measurement, (−) denotes model compounds not used for LCF.

Sample	Pyrite (%)	Elemental sulfur (%)	Sulfate (%)	FeS (%)	R-factor
Source rock	82(1)	0(< 1)	18 (< 1)	–	0.0077
Inoculated	86(1)	0(< 1)	7 (< 1)	7 (< 1)	0.0012
Uninoculated	90(2)	2(1)	7 (< 1)	–	0.0024

Table 3
Summary of Mössbauer results from spectra collected at 77 K.

Sample	Pyrite (% rel. Abund.)	Fe(II) mineral (% rel. Abund.)	Fe(II)-bearing phyllosil. (% rel. Abund.)
Source rock	29.5	31.0	39.5
Inoculated	29.2	33.8	37.0
Uninoculated	28.4	24.1	47.5

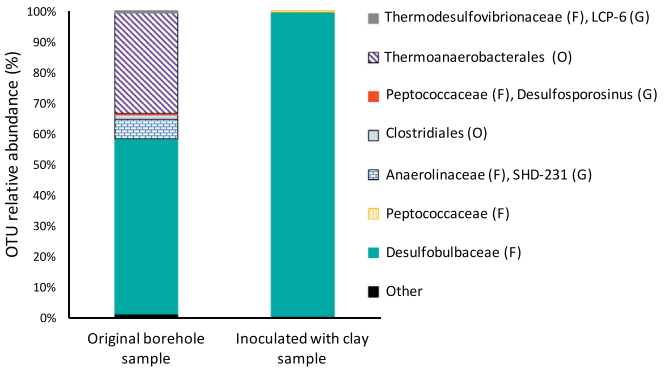

Fig. 3. Microbial community composition represented by the relative abundance of classified OTUs as a percentage of the total reads per sample. OTUs which accounted for < 0.005% of the total reads were grouped together as 'Other'. (O) – order; (F) – family; (G) – genus.

4. Discussion

The aim of this study was to determine the impact of SRB on the speciation of iron and sulfur in Opalinus Clay under DGR relevant conditions. The experimental results suggested that two major components were driving the geochemical changes. Firstly, changes to aqueous sulfate and iron concentrations occurred primarily in systems where clay was present, in contrast to solution-only systems which showed minimal variation for the duration of the experiment (Fig. 1). Sulfate was detected in the presence and absence of clay, indicating that both the Mont Terri porewater (used as inoculum) and the clay were sources of sulfate in these experiments (APW is devoid of sulfate). The highest concentration of sulfate was found in experiments with both clay and inoculum present. As the Opalinus Clay is known to contain trace amounts of celestite (Pearson et al., 2003), the dissolution of this phase would supply sulfate to the aqueous phase. According to geochemical speciation analyses, celestite was predicted to be undersaturated for the duration of the experiment (see supplementary information, S3). The results of the XANES analysis (Table 2) showed evidence for sulfate in the Opalinus Clay, with the highest proportion of sulfate found in the unaltered source rock (18%). After incubation, the proportion of sulfate in both inoculated and uninoculated solids was lower (7%), which is consistent with sulfate release into solution due to the purely abiotic dissolution of celestite as the clay rock equilibrated with the solution. More sulfate was observed in the incubations with higher Opalinus Clay content due to the near complete dissolution of celestite.

Fe^{2+} was not detected in solution in experiments where Opalinus Clay was absent, but was found in all experiments where it was present,

indicating that Opalinus Clay was the source of dissolved Fe^{2+} in the system. The results of the ^{57}Fe Mössbauer spectroscopy demonstrated that three phases, pyrite, an Fe(II)-bearing mineral, and an Fe(II)-bearing phyllosilicate, were the major Fe-containing phases within the Opalinus Clay with both phases identified in all three experimental samples (unaltered source rock, inoculated and uninoculated clay) with similar proportions found in the unaltered source rock and the incubated samples. The production of aqueous Fe^{2+} has been linked to active microbially mediated sulfate reduction in previous studies of bentonite (Pedersen et al., 2017), however, the results of the present study showed that, at the end of the experiments, the highest concentration of Fe^{2+} was found in experiments without inoculum suggesting that the release of Fe^{2+} was an abiotic reaction. The presence of Fe^{2+} in the aqueous phase was likely due to the partial dissolution of the Fe(II)-containing minerals. In previous studies, siderite was found to be a major Fe(II) mineral in Opalinus clay (Pearson et al.,2003), and could be a potential candidate for the Fe(II) mineral phase identified by Mössbauer spectroscopy. A PHREEQC model showed both Fe^{2+} and SO_4^{2-} in solution (6×10^{-5} and 7×10^{-4} mol/L respectively) when the solution was equilibrated with siderite, pyrite and celestite and no microbial activity was present (see SI, section S2). The concentration of Fe^{2+} also increased throughout the duration of the experiments where microbial activity was present, although it remained lower than in the experiments without microbial activity. The Fe^{2+} concentration of the 20 g*L^{-1} uninoculated experiment showed some variation with 0 µM recorded on day 47, however this was followed by a consistent increase in Fe^{2+} concentration for the remainder of the experiment and so is assumed to be an experimental artefact. There was a difference in concentration between the uninoculated experiments with clay present, in which a much higher concentration was found at the end of the 40 g*L^{-1} experiment than the 20 g*L^{-1} (85 and 47 µM respectively, Fig. 1g,h) which could be due to the higher rate of siderite dissolution in the 40 g*L^{-1} system due to the larger surface area available for the reaction to occur.

The second driver of geochemical change was microbial activity: borehole water from Mont Terri, including the associated microbial community, was used to inoculate experiments. Where inoculum was present, the sulfate concentration decreased rapidly (Fig. 1a,b), while uninoculated samples showed minimal changes in sulfate concentration over time suggesting that it was the microbial activity which was responsible for the reduction of sulfate (Canfield, 2001a, 2001b). Because there was no evidence for sulfate reduction in the absence of the porewater amendment, we conclude that the porewater rather than the clay itself was the source of sulfate-reducing bacteria (Fig. 1). The absence of sulfate reduction in the no-clay control that received inoculum from the porewater was due to the lack of clay. The clay acted as a reducing agent because of the presence of minerals such as siderite and pyrite (Mazurek, 1999; Thury and Bossart, 1999). Hence in that control, high redox conditions persisted for a long time, precluding sulfate reduction. Results from the 16S rRNA sequencing showed the dominance of known SRB with over 98% of reads from the inoculated sample being classified to the *Desulfobulbaceae* family. This family consists of strict anaerobes, and most members are mesophilic SRB with some species able to utilize H_2 as an electron donor (Kuever, 2014). The 16S rRNA results support the findings of previous subsurface investigations at this site which found that SRB are often the largest group within the community (Bagnoud et al., 2016a, 2016b, 2016c; Leupin et al., 2017). Insufficient DNA product was found in uninoculated samples, suggesting that there was limited, if any, microbial activity within these samples. In all experiments, including those without clay, there was a slight increase in the pH value followed by a decrease. These fluctuations may be due to an initial outgassing of CO_2 from solution and continuing equilibration with the N_2:H_2 headspace in the experiment bottles.

In Eq. (1), the reduction of sulfate produced aqueous sulfide, however none was measured in the experiments with microbial activity even though the sulfate concentration was decreasing (Fig. 1). Hence, sulfide must have precipitated out of the aqueous phase. A previous study (Pedersen et al., (2017)) proposed a coupled reaction of reducing Fe(III)(s) to Fe^{2+}(aq) and partially oxidizing HS^-(aq) to S^0(s) within bentonite (see Eq. (2)). No Fe(III)-containing iron oxide minerals were detected in the Opalinus Clay samples used in this study, although illite has been identified using EXAFS analysis (see supplementary information, Section S6). Illite can contain up to 80% of Fe as Fe(III), some of which may be available for reduction by HS^- (Dong et al., 2003; Liu et al., 2017; Lohmayer et al., 2014). Although increasing aqueous Fe^{2+} concentrations were recorded in this study, there was no evidence that this was as a result of S^0 formation in Opalinus Clay as no S^0 was found within the solid phase at the end of the inoculated experiment. Thus, any Fe(III) that might be held within the phyllosilicate clay minerals did not appear to be available for reaction with HS^-. The absence of HS^- in solution therefore was more likely to be due to the reaction between the HS^- and Fe^{2+} to form iron sulfide precipitates (Eq. (3)). The results of the solid phase Fe analysis showed minimal differences between the unaltered source rock and the incubated samples, but this is likely due to the fact that only a small fraction of the total iron pool was reacting.

In contrast, the results of the S XANES highlighted changes to the Opalinus Clay after incubation. The reduction of the proportion of sulfate within both clay samples after incubation was expected due to the corresponding increase in concentration in aqueous sulfate. The results of the inoculated sample show that FeS was present which was not found in the other samples, supporting the proposed reaction of HS^- and Fe^{2+} in solution to form both FeS and perhaps FeS_2 (pyrite) precipitates (Fig. 4). This resulted in a lack of HS^- in solution as evidenced in these experiments and also explained why the Fe^{2+}(aq) concentration remained higher in uninoculated samples where there was no HS^- to react with Fe^{2+}. The results also showed a higher percentage of pyrite in the uninoculated sample than both the unaltered source rock and the inoculated sample. This may be a proportional effect as the uninoculated sample is expected to have a reduced total sulfur content in the solid phase in comparison to the unaltered source rock and the inoculated samples equivalent to approximately 3% reduction in total sulfur concentration (see supplementary information, S8 for calculation). In the uninoculated sample, the dissolution of $SrSO_4$ (celestite) reduced the total sulfur concentration in the solid phase compared to both the source rock and the inoculated sample. There is also some heterogeneity within the Opalinus Clay which may result in varying total sulfur concentrations within clay samples. The ^{57}Fe Mössbauer results (Table 3) did not show any change in proportion of pyrite between all three samples which supports the assumption that this result is due to the changes in total sulfur concentration in the solid phase. The results of the uninoculated sample suggest the presence of a small amount of S_0 which was not found in the other samples, however

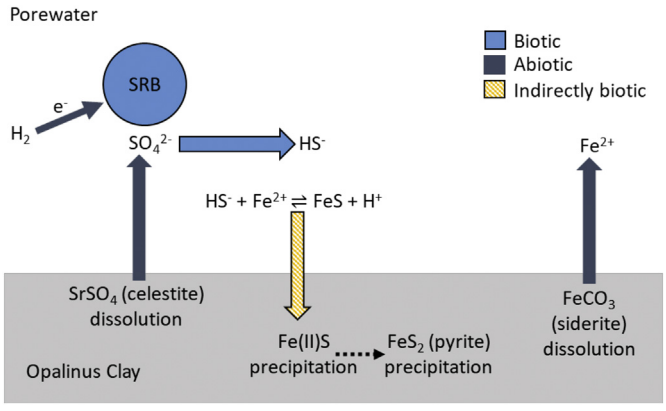

Fig. 4. Summary diagram of proposed interaction of sulfate-reducing bacteria and Opalinus Clay.

S_0 has been detected in Opalinus Clay at Mont Terri URL previously (Pearson et al., 2003).

In summary, Fe^{2+} was released into solution due to the dissolution of Fe(II)-bearing phases, which is supported by the evidence of aqueous Fe^{2+} in all experiments where Opalinus Clay was present and by the PHREEQC model. The initial concentration of aqueous sulfate was also due to dissolution of minerals, most likely celestite, as suggested by the presence of sulfate in microcosms where clay was present. Where inoculum was added, there was a rapid decrease in sulfate concentration as it was utilized by sulfate-reducing microorganisms with H_2 as the electron donor, confirming previous findings (Bagnoud et al., 2016a). There was no evidence for the formation of elemental sulfur in these experiments, instead it appears that HS^- produced from sulfate reduction reacted with Fe^{2+} to form FeS (based on the LCF of XANES results).

In this study, sulfate concentrations were artificially minimized by removing all sulfate from the artificial porewater composition to better deconvolute the possible formation of elemental sulfur (which would not be detectable if large amounts of FeS were formed). Naturally occurring sulfate concentrations in Opalinus Clay porewater are ~24 mM (Bagnoud et al., 2016a) while the maximum initial aqueous sulfate concentration in this study was ~0.8 mM and resulted from the porewater used as inoculum. Under water-saturated conditions, the potential HS^- concentration would therefore be much higher *in-situ* and the aqueous Fe^{2+} would be depleted as seen by Bagnoud et al., (2016a), diminishing the protective impact the iron sulfide precipitation reaction may have on the canister lifetime. A corresponding higher Fe^{2+} concentration would be necessary to maximise the amount of iron sulfide precipitation where high sulfate concentrations are naturally occurring. It is therefore also important to identify potential impacts of FeS precipitation, particularly with regards to clay swelling. Previous research found that microbially-mediated FeS precipitation led to a decrease in the swelling capacity and water retention of bentonite (Stone et al., 2016) which would be detrimental to a DGR environment. However, in the nuclear waste repository environment, it is presently unknown whether sulfate reduction will occur in a sustained manner, depending on the amount of space and water available. Whether there would be sufficient dissolution of Fe^{2+} from the source rock to ensure the FeS precipitation *in-situ* in the long-term is also a question that needs further investigation.

5. Conclusion

This study provides evidence that microbial activity in the form of sulfate-reducing bacteria has the potential to influence a DGR environment provided there is sufficient space and water activity. The hydrogen gas which is predicted to form from corrosion can be utilized by the sulfate-reducing bacteria within the porewater of the Opalinus Clay. There was no evidence in this study that sulfate-reducing bacteria were supplied from the solid clay phase. The hydrogen sulfide produced will be retained in the solid phase as iron sulfide minerals where sufficient Fe^{2+} is available. Sustained microbial sulfate reduction and the associated precipitation of FeS could enhance the long-term integrity of the repository by reducing the gas pressure and by removing corrosive sulfide from solution.

Declarations of interest

None.

Acknowledgements

This project has received funding from the Euratom, (EU) research and training programme 2014-2018 MIND project under grant agreement (No 661880). In addition, this work was supported by the Swiss State Secretariat for Education, Research and Innovation (SERI), Switzerland under contract number (15.0177). The opinions expressed and arguments employed herein do not necessarily reflect the views of the Swiss Government.

We would like to acknowledge Maria Pilar Asta Andres for the collection of sulfur XANES spectra and help with LCF fitting of iron EXAFS spectra. The S K-edge and Fe K-edge XAS experiments were performed on the 4-3 and the 4-1 beamline at the Stanford Synchrotron Radiation Lightsource (SSRL). We are grateful for the technical assistance received during the XAS analyses from Ryan Davis, Erik Nelson and Matthew Latimer. Use of the SSRL, SLAC National Accelerator Laboratory is supported by the US Department of Energy, USA, Office of Science, Office of Basic Energy Sciences under Contract (DE-AC02076SF00515).

Appendix A. Supplementary data

Supplementary data to this article can be found online at https://doi.org/10.1016/j.clay.2019.03.020.

References

Bagnoud, A., Chourey, K., Hettich, R.L., De Bruijn, I., Andersson, A.F., Leupin, O.X., Schwyn, B., Bernier-Latmani, R., 2016a. Reconstructing a hydrogen-driven microbial metabolic network in Opalinus Clay rock. Nat. Commun. 7 (12770). https://doi.org/10.1038/ncomms12770.

Bagnoud, A., de Bruijn, I., Andersson, A.F., Diomidis, N., Leupin, O.X., Schwyn, B., Bernier-Latmani, R., 2016b. A minimalistic microbial food web in an excavated deep subsurface clay rock. FEMS Microbiol. Ecol. 92, 1–12. https://doi.org/10.1093/femsec/fiv138.

Bagnoud, A., Leupin, O., Schwyn, B., Bernier-Latmani, R., 2016c. Rates of microbial hydrogen oxidation and sulfate reduction in Opalinus Clay rock. Appl. Geochem. 72, 42–50. https://doi.org/10.1016/j.apgeochem.2016.06.011.

Bengtsson, A., Pedersen, K., 2016. Microbial sulphate-reducing activity over load pressure and density in water saturated Boom Clay. Appl. Clay Sci. 132–133, 542–551. https://doi.org/10.1016/j.clay.2016.08.002.

Canfield, D.E., 2001a. Biogeochemistry of Sulfur Isotopes. Rev. Mineral. Geochem. 43, 607–636.

Canfield, D.E., 2001b. Isotope fractionation by natural populations of sulfate-reducing bacteria. Geochim. Cosmochim. Acta 65, 1117–1124. https://doi.org/10.1016/S0016-7037(00)00584-6.

Cline, J.D., 1969. Spectrophotometric determination of hydrogen sulfide in natural waters. Limnol. Oceanogr. 14, 454–458.

Dong, H., Kukkadapu, R.K., Fredrickson, J.K., Zachara, J.M., Kennedy, D.W., Kostandarithes, H.M., 2003. Microbial reduction of structural Fe(III) in illite and goethite. Environ. Sci. Technol. 37, 1268–1276. https://doi.org/10.1021/es020919d.

Houben, M.E., Desbois, G., Urai, J.L., 2014. A comparative study of representative 2D microstructures in Shaly and Sandy facies of Opalinus Clay (Mont Terri, Switzerland) inferred form BIB-SEM and MIP methods. Mar. Pet. Geol. https://doi.org/10.1016/j.marpetgeo.2013.10.009.

IAEA, 2003. Scientific and Technical Basis for the Geological Disposal of Radioactive Wastes, No. 413. Vienna.

Kostka, J.E., Wu, J., Nealson, K.H., Stucki, J.W., 1999. The impact of structural Fe(III) reduction by bacteria on the surface chemistry of smectite clay minerals. Geochim. Cosmochim. Acta 63, 3705–3713. https://doi.org/10.1016/S0016-7037(99)00199-4.

Kuever, J., 2014. The Family Desulfobulbaceae. In: Rosenberg, E., DeLong, E.F., Lory, S., Stackebrandt, E., Thompson, F. (Eds.), The Prokaryotes: Deltaproteobacteria and Epsilonproteobacteria. Springer Berlin Heidelberg, Berlin, Heidelberg, pp. 75–86. https://doi.org/10.1007/978-3-642-39044-9_267.

Lantenois, S., Lanson, B., Muller, F., Bauer, A., Jullien, M., Plançon, A., 2005. Experimental Study of Smectite Interaction with Metal Fe at Low Temperature: 1. Smectite destabilization, Clays and Clay Minerals - CLAYS CLAY MINERhttps://doi.org/10.1346/CCMN.2005.0530606.

Leupin, O.X., Bernier-Latmani, R., Bagnoud, A., Moors, H., Leys, N., Wouters, K., Stroes-Gascoyne, S., 2017. Fifteen years of microbiological investigation in Opalinus Clay at the Mont Terri rock laboratory (Switzerland). Swiss J. Geosci. 110, 343–354. https://doi.org/10.1007/s00015-016-0255-y.

Libert, M., Bildstein, O., Esnault, L., Jullien, M., Sellier, R., 2011. Molecular hydrogen: an abundant energy source for bacterial activity in nuclear waste repositories. Phys. Chem. Earth 36, 1616–1623. https://doi.org/10.1016/j.pce.2011.10.010.

Lin, L.H., Hall, J., Lippmann-Pipke, J., Ward, J.A., Lollar, B.S., DeFlaun, M., Rothmel, R., Moser, D., Gihring, T.M., Mislowack, B., Onstott, T.C., 2005a. Radiolytic H2 in continental crust: Nuclear power for deep subsurface microbial communities. Geochem. Geophys. Geosyst. 6. https://doi.org/10.1029/2004GC000907.

Lin, L.H., Slater, G.F., Sherwood Lollar, B., Lacrampe-Couloume, G., Onstott, T.C., 2005b. The yield and isotopic composition of radiolytic H2, a potential energy source for the deep subsurface biosphere. Geochim. Cosmochim. Acta 69, 893–903. https://doi.org/10.1016/j.gca.2004.07.032.

Liu, G., Qiu, S., Liu, B., Pu, Y., Gao, Z., Wang, J., Jin, R., Zhou, J., 2017. Microbial

reduction of Fe(III)-bearing clay minerals in the presence of humic acids. Sci. Rep. 7, 45354.
Lohmayer, R., Kappler, A., Lösekann-Behrens, T., Planer-Friedrich, B., 2014. Sulfur Species as Redox Partners and Electron Shuttles for Ferrihydrite Reduction by Sulfurospirillum deleyianum. Appl. Environ. Microbiol. 80, 3141–3149. https://doi.org/10.1128/AEM.04220-13.
Lunau, M., Lemke, A., Walther, K., Martens-Habbena, W., Simon, M., 2005. An improved method for counting bacteria from sediments and turbid environments by epifluorescence microscopy. Environ. Microbiol. 7, 961–968. https://doi.org/10.1111/j.1462-2920.2005.00767.x.
Mazurek, M., 1999. Mineralogy of the Opalinus Clay. In: Thury, M., Bossart, P. (Eds.), Mont Terri Rock Laboratory: Results of the Hydrogeological, Geochemical and Geotechnical Experiments Performed in 1996 and 1997. Vol 23. Federal Office of Topography Swisstopo, Bern, pp. 15–18.
Nagra, 2002. Project Opalinus Clay. Safety report. Demonstration of disposal feasibility for spent fuel, vitrified high-level waste and long-lived intermediate-level waste (Entsorgungs- nachweis). Report NTB 02–05.
Nagra, 2008. Vorschlag geologischer Standortgebiete für das SMA- und das HAA-Lager. Darlegung der Anforderungen, des Vorgehens und der Ergebnisse (Hauptbericht). Nagra Tech. Rep. NTB 08–03.
NCRP, 1978. Handbook of Radioactivity Measurements Procedures: with nuclear data for some biologically important radionuclides: recommendations of the National Council on Radiation Protection and Measurements. NCRP (National Council on Radiation Protection and Measurements (U.S.)).
Parkhurst, D.L., Appelo, C.A.J., 2013. Description of Input and Examples for PHREEQC Version 3: A Computer Program for Speciation, Batch-Reaction, One-Dimensional Transport, and Inverse Geochemical Calculations. (US Geological Survey).
Pearson, F.J., Arcos, D., Bath, A., Boisson, J.Y., Fernández, A.M., Gäbler, H.E., Gaucher, E., Gautschi, A., Griffault, L., Hernán, P., Waber, H.N., 2003. Mont Terri Project – Geochemistry of Water in the Opalinus Clay Formation at the Mont Terri Rock Laboratory. Geol. Ser. 10, 321.
Pedersen, K., Bengtsson, A., Blom, A., Johansson, L., Taborowski, T., 2017. Mobility and reactivity of sulphide in bentonite clays - Implications for engineered bentonite barriers in geological repositories for radioactive wastes. Appl. Clay Sci. 146, 495–502. https://doi.org/10.1016/j.clay.2017.07.003.
Pentráková, L., Su, K., Pentrák, M., Stucki, J.W., 2013. A review of microbial redox interactions with structural Fe in clay minerals. Clay Miner. 48, 543–560.
Pyzik, A.J., Sommer, S.E., 1981. Sedimentary iron monosulfides: Kinetics and mechanism of formation. Geochim. Cosmochim. Acta 45, 687–698. https://doi.org/10.1016/0016-7037(81)90042-9.
Rancourt, D.G., Ping, J.Y., 1991. Voigt-based methods for arbitrary-shape static hyperfine parameter distributions in Mössbauer spectroscopy. Nucl. Instruments Methods Phys. Res. Sect. B Beam Interact. with Mater. Atoms 58, 85–97.
Ravel, B., Newville, M., 2005. Athena, Artemis, Hephaestus: data analysis for X-ray absorption spectroscopy using IFEFFIT. J. Synchrotron Radiat. 12, 537–541.
Smart, N.R., Blackwood, D.J., Werme, L., 2001. The Anaerobic Corrosion of Carbon Steel and Cast Iron in Artificial Groundwaters. Swedish Nuclear Fuel and Waste Management Co.
Stone, W., Kroukamp, O., Mckelvie, J., Korber, D.R., Wolfaardt, G.M., 2016. Applied Clay Science Microbial metabolism in bentonite clay : Saturation, desiccation and relative humidity. Appl. Clay Sci. 129, 54–64. https://doi.org/10.1016/j.clay.2016.04.022.
Stookey, L.L., 1970. Ferrozine—a new spectrophotometric reagent for iron. Anal. Chem. 42, 779–781. https://doi.org/10.1021/ac60289a016.
Stroes-Gascoyne, S., Schippers, A., Schwyn, B., Poulain, S., Sergeant, C., Simonoff, M., Le Marrec, C., Altmann, S., Nagaoka, T., Mauclaire, L., 2007. Microbial community analysis of Opalinus clay drill core samples from the Mont Terri underground research laboratory, Switzerland. Geomicrobiol J. 24, 1–17. https://doi.org/10.1080/01490450601134275.
STUK, 2017. Disposal of Spent Fuel in Finland WWW Document. http://www.stuk.fi/web/en/topics/nuclear-waste/disposal-of-spent-fuel-in-finland (accessed 1.8.18).
Thury, M., 2002. The characteristics of the Opalinus Clay investigated in the Mont Terri underground rock laboratory in Switzerland. Comptes Rendus Phys. 3, 923–933. https://doi.org/10.1016/S1631-0705(02)01372-5.
Thury, M., Bossart, P., 1999. The Mont Terri rock laboratory, a new international research project in a Mesozoic shale formation, in Switzerland. 52. pp. 347–359.
Vinsot, A., Appelo, C.a.J., Lundy, M., Wechner, S., Lettry, Y., Lerouge, C., Fernandez, a.M., Labat, M., Tournassat, C., De Canniere, P., Schwyn, B., Mckelvie, J., Dewonck, S., Bossart, P., Delay, J., 2014. In situ diffusion test of hydrogen gas in the Opalinus Clay. Geol. Soc. London, Spec. Publ. 400, 563–578. https://doi.org/10.1144/SP400.12.
Vladimir, V., Igor, S., 2009. Applied Biophysics of Activated Water: The Physical Properties, Biological Effects and Medical Applications of Mret Activated Water. World Scientific Publishing Company.